



## Search for Lorentz Invariance Violation with flaring Active Galactic Nuclei: a prospect for the Cherenkov Telescope Array

J. BOLMONT<sup>1</sup>, D. EMMANOULOPOULOS<sup>2</sup>, A. JACHOLKOWSKA<sup>1</sup>, J.-P. TAVERNET<sup>1</sup> FOR THE CTA CONSORTIUM  
<sup>1</sup>LPNHE, Université Pierre et Marie Curie Paris 6, Université Denis Diderot Paris 7, CNRS/IN2P3, 4 Place Jussieu, F-75252, Paris Cedex 5, France

<sup>2</sup>School of Physics and Astronomy, University of Southampton, SO17 1BJ Southampton, United Kingdom  
 bolmont@in2p3.fr DOI: 10.7529/ICRC2011/V08/0883

**Abstract:** In the recent years, many results have been published about a possible violation of Lorentz Invariance in the frame of Quantum Gravity (QG) models measuring time delays in the arrival times of very high energy (VHE, >100 GeV) gamma-ray photons from distant flaring active galaxies. These photons have been detected by the current ground-based VHE Cherenkov detectors (HESS, MAGIC, VERITAS) and so far, no deviations in the speed of light in vacuum have been seen either for linear or for quadratic scales. The new generation of ground-based instruments "the Cherenkov Telescope Array" (CTA) will be able to probe deeper into this area due to its increased sensitivity (one order of magnitude better than the current detectors) and broader energy range (above 10 GeV). Based on a maximum likelihood technique, a quantitative study is presented of the potential of CTA to detect possible QG effects. In addition, different array configurations are compared in an attempt to maximize the sensitivity to Lorentz Invariance Violation (LIV) effects.

**Keywords:** CTA, active galaxies, Quantum Gravity, Lorentz Invariance Violation

### 1 Quantum Gravity and Lorentz Invariance Violation

The search for a quantum theory of gravitation is one of the outstanding tasks of modern physics [1]. As an important consequence of the time-space discretization, Lorentz Invariance Violation (LIV) may appear as predicted in some models of Loop Quantum Gravity [2] or String Theory [3]. The tiny effects in the photon propagation from distant astrophysical sources as Active Galactic Nuclei (AGNs) or Gamma-ray Bursts (GRBs) would add-up producing deviations in the value of the velocity of light [4]. These deviations could be represented by linear and quadratic terms in the so-called dispersion relation:

$$c^2 p^2 = E^2 (1 \pm \xi(E/M) \pm \zeta(E/M)^2 \pm \dots), \quad (1)$$

where  $M$  is the Quantum Gravity energy scale (in principle close to the Planck scale) and  $\xi$  and  $\zeta$  are positive parameters.

In this paper a search for LIV with photons emitted in flares of AGN is being presented as a prospect for the future Cherenkov Telescope Array (CTA) [5]. In section 2, the performance of the different possible array configurations, currently under evaluation with Monte Carlo simulations, are compared with the aim of maximizing the sensitivity to LIV effects. Then in section 3, the effect of potentially improved statistical accuracy due to both increased sensitivity and better energy coverage is evaluated.

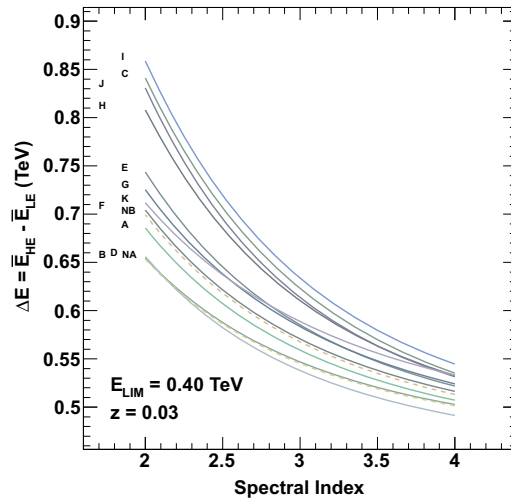


Figure 1: Parameter  $\Delta E$  as a function of the spectral index for all arrays considered in CTA Monte Carlo simulations. The configurations A to K are studied for Southern array and configurations NA and NB for the Northern array. The configurations have different layouts and number of telescopes [5].

### 2 Comparison of array configurations

The energy lever-arm  $\Delta E$  is determined in order to compare the different array configurations, following to the

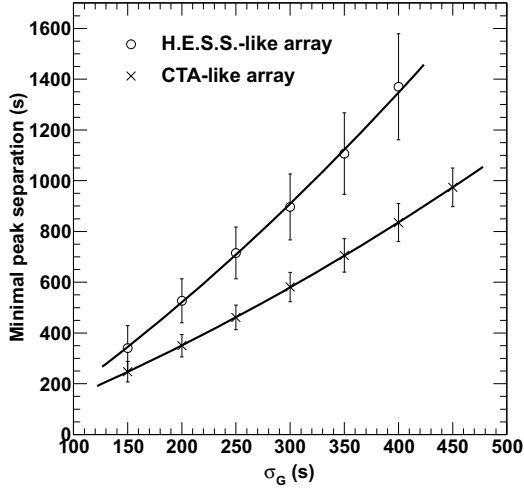


Figure 2: Minimal distinguishable separation of the two peaks as a function of their width, in case of a H.E.S.S.-like (open circles) and a CTA-like measurement (crosses).

spectrum simulation of a power law with EBL absorption [11] (for a redshift  $z = 0.03$ ) and a break at 100 GeV representing the maximum of the Inverse Compton peak. The spectrum is then convoluted with the effective areas of different array configurations. Finally, the mean energy for low ( $E < E_{lim}$ ) and high ( $E > E_{lim}$ ) energy bands are computed and the difference  $\Delta E = \bar{E}_{HE} - \bar{E}_{LE}$  is deduced. This way of comparing the different array configurations does not depend on the method used to compute the time lags.

Fig. 1 shows the parameter  $\Delta E$  as a function of the spectral index for all arrays considered in CTA Monte Carlo simulations.  $E_{lim}$  is chosen to be optimal while preserving the highest statistics at high energies. This value is almost stable regardless of the array or spectral index used and lies around 500 GeV. Arrays which maximize  $\Delta E$  are J, C, H, I for the Southern site and NB for the Northern array. The same ranking is obtained for the quadratic difference  $\Delta E^2$ .

### 3 Effect of increased statistics

#### 3.1 The analysis procedure

Here a likelihood fit procedure, as described in detail in [6, 7], is used to measure the energy dependant time lags. This method makes use of individual photon information (energy and detection time) and requires a parameterization of both the light curve and the spectrum. The light curve is parameterized (function  $F_S$ ) at low energies where the time lags are supposed to be negligible and the measured spectrum ( $\Lambda$ ) is parameterized in the full energy range of the instrument. Then the probability density function (pdf)

is given by:

$$P(t, E) = \int_0^\infty \Lambda(E_S) G(E - E_S, \sigma(E_S)) F_S(t - \tau_l E_S) dE_S, \quad (2)$$

where  $G$  takes into account the energy resolution of the detector, considered here to be 10%. After normalizing the pdf, the parameter  $\tau_l$  (here for the linear correction to the dispersion relation of Eq. 1) is obtained by minimizing  $-\ln(L)$  where

$$L = \prod_{\text{all photons}} P(t, E). \quad (3)$$

A toy Monte Carlo software developed for PKS 2155-304 analysis [6] is used to simulate various sets of photons with given time and energy distributions. The injected lags range from  $-60 \text{ s TeV}^{-1}$  to  $60 \text{ s TeV}^{-1}$  in steps of  $20 \text{ s TeV}^{-1}$  for the linear case and from  $-60 \text{ s TeV}^{-2}$  to  $60 \text{ s TeV}^{-2}$  in steps of  $20 \text{ s TeV}^{-2}$  for the quadratic case. For each injected lag, 500 realizations of the lightcurve are simulated. The obtained distribution of reconstructed lags is a Gaussian with standard deviation  $\sigma_\tau$ . The mean dispersion  $\bar{\sigma}_\tau$  is the average of  $\sigma_\tau$  for all injected lags.

#### 3.2 Peak separation capabilities

The likelihood fit procedure requires the measured light curve to be parameterized at low energies. As the error  $\sigma_\tau$  is smaller when the spikes of the light curve are narrower, the peak separation capability is essential: a single peak seen by present day experiments could be observed with sub-structures with an instrument as CTA, which would in turn increase the performance of the analysis. In this section, this issue is studied using simple hypotheses.

A list of 3000 photons is generated randomly with energies following a power law distribution with index  $\Gamma = 2.8$  and a time distribution chosen to be the sum of two Gaussian functions, which have the same standard deviation  $\sigma_G$  and the separation between the peaks is varied from 0 to 1400 s. The time distribution is fitted with one or two Gaussian functions. The bin width of the light curve is set to 60 s for H.E.S.S./MAGIC and to 30 s for CTA. The minimal peak separation is then obtained when  $\chi^2/\text{dof} = 1.5$ .

Fig. 2 shows the minimal peak separation necessary to distinguish the two spikes as a function of  $\sigma_G$ . For example, for two spikes of width  $\sigma_G = 300 \text{ s}$ , a separation of at least 900 s is needed for H.E.S.S./MAGIC and only 500 s for CTA.

In order to quantify the effect of this result on the limits on  $M_{LIV}$ , the likelihood was computed for  $\sigma_G = 300 \text{ s}$  and a peak separation of 700 s.

As an example of this type of studies, Fig. 3 (next page) shows the fit of a realization of the light curve (left) and the distribution of likelihood minima for 1000 realizations (right) for an injected lag of  $0 \text{ s TeV}^{-1}$  and for 300 photons.

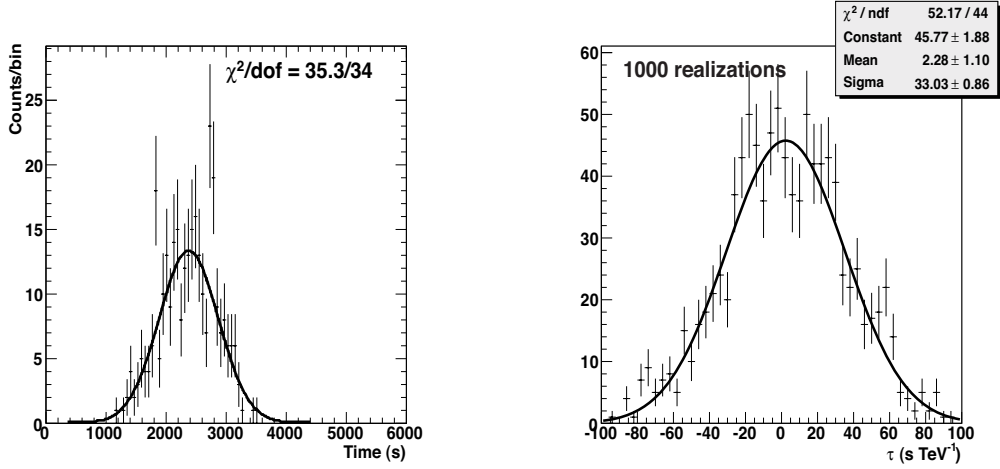


Figure 3: Left: realization of a light curve with 300 photons and a binning of 60 s (H.E.S.S. case). The fit with a Gaussian curve leads to  $\chi^2/\text{dof} = 35.3/34$ . Right: distribution of the minimum of the likelihood for 1000 realizations of the lightcurve. The distribution is fitted with a Gaussian curve.

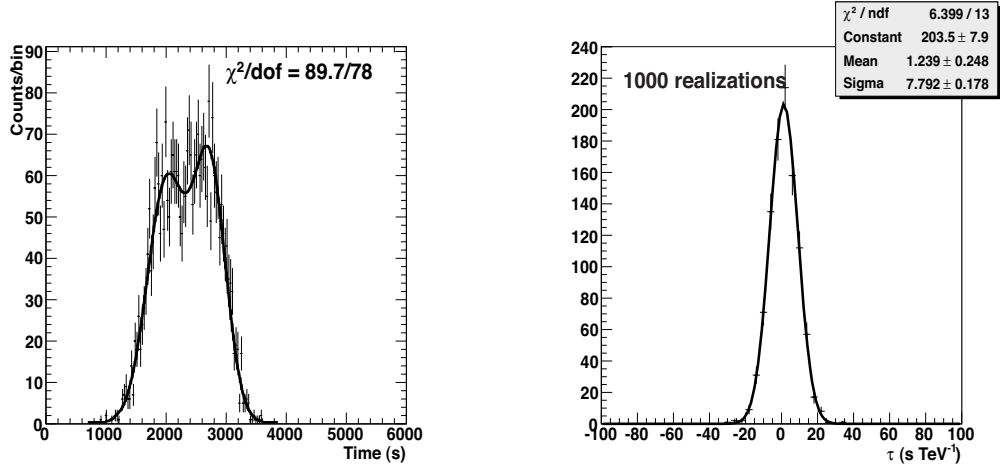


Figure 4: Left: the flare of Fig. 3 (left) with 3000 photons and a binning of 30 s (CTA case). The fit with a double Gaussian curve leads to  $\chi^2/\text{dof} = 89.7/78$ . Right: distribution of the minimum of the likelihood for 1000 realizations of the lightcurve. The distribution is fitted with a Gaussian curve.

The fit of the lightcurve with a single Gaussian curve gives a good value of  $\chi^2/\text{dof} = 35.3/34$ .

Fig. 4 shows the same plots for 3000 photons. The two peaks are clearly visible and the light curve is fitted with the sum of two Gaussian functions. The lag reconstruction precision is improved by a factor of 5.

### 3.3 Lag reconstruction precision

The time distribution of photons is considered to be a Gaussian curve with a standard deviation of  $\sigma_P$ . The energy distribution follows a power law  $E^{-\Gamma}$  with index taking discrete values from  $\Gamma = 2.2$  (Mkn 501, MAGIC [8]) to  $\Gamma = 3.4$  (PKS 2155-304, H.E.S.S. [9]).

Fig. 5 (left) shows the average error  $\bar{\sigma}_\tau$  on the reconstructed lag as a function of the number  $N_L$  of photons included in the likelihood fit computation *ie* photons in the energy range of 0.3–10 TeV. As expected, the error on reconstructed lags follows the relation:

$$\bar{\sigma}_\tau \sim 1/\sqrt{N}. \quad (4)$$

When the width of the light curve peak  $\sigma_P$  increases from 100 s to 500 s,  $\bar{\sigma}_\tau$  increases as well. This is related to the fact that the error on the lag is strongly dependent on the variability amplitude of the source.

Fig. 5 (right) shows the mean error  $\bar{\sigma}_\tau$  on the reconstructed lag as a function of the number  $N_L$  of photons included in the likelihood fit calculation for three different values of the spectral index  $\Gamma = 3.4, 2.8$  and  $2.2$  for the linear and

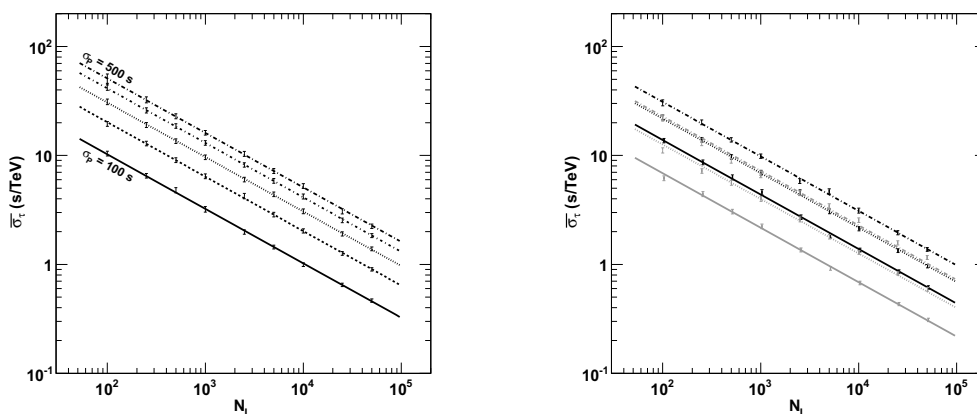


Figure 5: Average error on the reconstructed lag as a function of the number of photons used in the likelihood fit computation. Points are fitted with the function defined in Eq. 4. Left: the different set of points correspond to different light curve peak widths: from bottom to top,  $\sigma_P = \{100, 200, 300, 400, 500\}$ . Right: Black and gray lines correspond respectively to linear and quadratic effects. Dash-dotted, dotted and solid lines correspond respectively to  $\Gamma = 3.4, 2.8$  and  $2.2$ .

quadratic models. Here again, the error on reconstructed lags follows the relation of Eq. 4. This figure also illustrates the fact that harder spectra favour the detection of possible quadratic effects.

As a conclusion at this step, it is expected that a flare like the one of PKS 2155-304 in July 2006 would lead to an error of  $<1 \text{ s TeV}^{-1}$  (considering systematic and statistical effects) with CTA.

## 4 Discussion

The simulations performed for this work show that CTA will greatly improve the sensitivity of photon propagation studies with respect to LIV effects. Considering the fact that the sensitivity will be ten times better than the one of present-day experiments and that the energy range covered will be much larger, the Planck scale will be easily reached for the “linear” models, conforing the present *Fermi* and H.E.S.S. results [12, 13, 6]. In case of a flare as the one of Mkn 501 seen by MAGIC, Planck scale will be reached for the linear correction to the dispersion relations while a flare as the one seen by H.E.S.S. with PKS 2155-304 would largely exceed this value. The main increase in sensitivity will be reflected in the LIV scale in case of the “quadratic” models where a new range of detection will emerge. In particular, taking into account the best array configurations of section 2, the limits for the quadratic term of the dispersion relation should be higher than  $10^{12} \text{ GeV}$ .

Another important question for future studies is how many AGN flares will be observed by CTA. Of all flares observed so far, only three had enough statistics and high variability to be used for search of LIV. It is expected that CTA will detect tens of AGN flares per year, especially in the so-called “survey pointing mode” where each telescope aims at different locations of the sky, allowing a higher probab-

ity to detect transient events. This will allow to increase the sensitivity to LIV effects by use of stacking procedures.

## Acknowledgments

We gratefully acknowledge support from the agencies and organizations listed in this page: [http://www.cta-observatory.org/ctawpcwiki/images/5/5b/Acknowledgement\\_CTA.Short.txt](http://www.cta-observatory.org/ctawpcwiki/images/5/5b/Acknowledgement_CTA.Short.txt). DE acknowledges the Science and Technology Facilities Council (STFC) for support under grant ST/G003084/1. AJ and JB acknowledges the support of GdR PCHE in France.

## References

- [1] Amelino-Camelia, 2008, arXiv:0806.0339
- [2] Alfaro, J. et al., Phys. Rev. D, 2002, **65**, 103509; Gambini & Pullin, Phys. Rev. D, 1999, **59**, 124021
- [3] Ellis, Mavromatos, Nanopoulos, Phys. Rev. D, 1999, **61**, 027503
- [4] Amelino-Camelia, G. et al., Nature, 1998, **395**, 525
- [5] CTA Consortium, arXiv:1008.3703, 2010; <http://www.cta-observatory.org>
- [6] H.E.S.S. Collaboration, Astropart. Phys., 2011, **34**, 738
- [7] Martinez & Errando, Astropart. Phys., 2009, **31**, 226
- [8] MAGIC Collaboration, ApJ, 2007, **669**, 862
- [9] H.E.S.S. Collaboration, ApJL, 2007, **664**, L71
- [10] MAGIC Collaboration, Phys. Lett. B, 2008, **668**, 253
- [11] Mazin, 2008, in Proc. of the Conference “Science with the New Generation of High Energy Gamma-Ray Experiments”, ed. Scineghe
- [12] Fermi LAT Collaboration, Science Express, 2009, 02/19/2009
- [13] Fermi LAT Collaboration, Nature, 2009, **462**, 331